

Two Novel Proteins Bind Specifically to Trichosanthin on Choriocarcinoma Cell Membrane

Xuechun Xia¹, Fajian Hou², Jie Li¹, Yibao Ke¹ and Huiling Nie^{1,*}

¹Institute of Biochemistry and Cell Biology, Shanghai Institutes for Biological Sciences, Chinese Academy of Sciences, Shanghai 200031, China; and ²Department of Molecular Biology, University of Texas Southwestern Medical Center, Dallas, TX 75390-9148, USA

Received January 25, 2006; accepted February 12, 2006

Trichosanthin is the active protein component in the Chinese herb *Trichosanthes kirilowii*, which has distinct pharmacological properties. The cytotoxicity of trichosanthin was demonstrated by its selective inhibition of various choriocarcinoma cells. When Jar cells were treated with trichosanthin, the influx of calcium into the cells was observed by confocal laser scanning microscopy. When the distribution of trichosanthin-binding proteins on Jar cells was studied, two classes of binding sites for trichosanthin were shown by radioligand binding assay. Furthermore, the cytoplasmic membrane of Jar cells was biotinylated and the trichosanthin-binding proteins were isolated with trichosanthin-coupled Sepharose beads. Two protein bands with molecular masses of about 50 kDa and 60 kDa were revealed, further characterization of which should shed light on the mechanism of the selective cytotoxicity of trichosanthin to Jar cells.

Key words: cell surface biotinylation, choriocarcinoma cells, cytotoxicity, radioligand binding assay, trichosanthin.

Abbreviations: TCS, trichosanthin; RIP, ribosome-inactivating protein; MTT, 3-(4,5-dimethylthiazol-2-yl)-2,5-diphenyl-2H-tetrazolium bromide; ECL, enhanced chemical luminescence reagent; PLAP, placental alkaline phosphatase; Con A, concanavalin A.

Trichosanthin (TCS) was isolated from root tubers of *Trichosanthes kirilowii* Maximowicz, which is characterized as a type I ribosome-inactivating protein (RIP) (1, 2), showing a very high overall structural similarity to ricin A-chain. It catalyzes the cleavage of a specific N-glycosidic bond in 28S rRNA, which inhibits protein synthesis by preventing the 60S ribosomal subunit from interacting with elongation factors. This reaction was well established in rabbit reticulocyte lysate *in vitro*.

TCS has been identified as the active component in the Chinese herb Tian Hua Fen. Its medical application was described as early as the 3rd century and it is still being used clinically in China to induce abortions, particularly in the second trimester, and to treat diseases of trophoblastic origin such as hydatidiform moles, invasive moles, and choriocarcinoma (3–8). In the early 1990s, TCS was applied in the treatment for AIDS or AIDS-related complex in phase I and II studies (9, 10). However, the cytotoxicity of TCS is largely unknown, current studies of TCS being mainly focused on its distinct internalization and the intracellular routing for it to exert ribosome-inactivating ability in different cells.

TCS is very effective in inducing abortion (94% success rate) with mild side effects (11). The underlying mechanism was postulated to involve direct and specific injurious effects on human syncytiotrophoblasts in placental villi (12, 13). The observed injurious effect of TCS on trophoblasts and other cell types also demonstrated its selective cytotoxicity (6, 14). There is increasing evidence that TCS

binds specifically to sensitive cells. Studies on the interactions of TCS with a monolayer of phospholipid membrane indicated that TCS preferentially binds to negatively charged phospholipid-containing membranes (15). It was shown that the LDL receptor-related protein/ α_2 -macroglobulin receptor serves as a receptor for most RIPs (16), and binding of these proteins to the RIPs initiates receptor-mediated endocytosis. Internalization of TCS into cells of leukocyte origin is mediated by its interaction with chemokine receptors (17). In addition, there is evidence that TCS stimulates the production of reactive oxygen species in Jar cells, leading to apoptosis, and the interaction of TCS with a membrane-bound receptor might be involved (18).

The present study examined the selective cytotoxicity of TCS to cultured cells. The specific binding of TCS to Jar cells was demonstrated by flow cytometry assays and radioligand binding determination. Furthermore, TCS-binding proteins on the Jar cell membrane were isolated by use of TCS-Sepharose beads.

MATERIALS AND METHODS

Materials—3-(4,5-Dimethylthiazol-2-yl)-2,5-diphenyl-2H-tetrazolium bromide (MTT), enhanced chemical luminescence reagent (ECL), Con A Sepharose beads and rabbit anti-actin antibody were products of Sigma. Fluo-3 acetoxymethyl ester (fluo-3/AM) was obtained from Molecular Probes. Iodo-beads, Sulfo-NHS-LC-biotin and Immobilized monomeric avidin kit were products of Pierce. ¹²⁵I (NaI, 1 mCi) was a product of Amersham Corp. CNBr activated Sepharose 4B were purchased from Amersham Pharmacia Biotech. FITC-conjugated antibody against

*To whom correspondence should be addressed. E-mail: hlnie@sibs.ac.cn

rabbit IgG and HRP-conjugated streptavidin were purchased from Vector Laboratories. Anti-placental alkaline phosphatase (PLAP) rabbit polyclonal antibody was from NeoMarkers. Protein A-Sepharose suspension and protein G plus-agarose beads were from Calbiochem. Anti-CCR5 antibody (CTC8) was from R&D. Inc. Rabbit anti-TCS antibody was prepared from Chinese big ear rabbit using purified TCS as immunogen.

Cell Lines and Cell Culture—JEG-3 choriocarcinoma cells and mouse prostate cancer cell line RM-1 were grown in modified essential medium (MEM) (Gibco BRL) containing penicillin (100 U/ml), streptomycin (100 µg/ml) and 10% (v/v) fetal bovine serum (FBS) in a humidified atmosphere of 5% CO₂ at 37°C. Jar choriocarcinoma, Wish and THP-1 cells were cultured in RPMI-1640 medium (Gibco BRL) supplemented with 10% FBS, penicillin (100 U/ml), and streptomycin (100 µg/ml).

Cytotoxicity Assay—The MTT assay for measuring cytotoxicity and cell growth was performed as previously (19, 20). In brief, 100 µl of cell suspension (3×10^4 cells) was seeded into wells of 96-well tissue-culture plates containing the indicated concentrations of TCS and incubated for 48 h. Control cells were not treated with TCS. MTT (5 mg/ml final concentration) was added to each well, and after incubation for 4 h, the formazan crystals produced by viable cells were dissolved for 12 h in 100 µl of 10% SDS–50% DMF. The absorbance at 570 nm was measured. The viable cell number was expressed as a percentage of control cells.

Confocal Laser Scanning Microscopy—For fluorescence measurements, the cells were incubated in a standard solution containing 5 µM fluo-3/AM (ester form of Ca²⁺ indicator dye) in RPMI 1640 for 1 h at 37°C. After being rinsed three times with a Hepes solution, the cells were treated with 25 µg/ml TCS for 5 min. The images of [Ca²⁺] were recorded every 10 s for up to 10 min by confocal laser scanning microscopy, with excitation at 488 nm and emission at 525 nm.

Flow Cytometric Assay—Previously established methods were followed (21, 22). In brief, adherent cells were digested with trypsin (0.25%)-EDTA (0.03%) solution, washed twice and resuspended in PBS (1×10^6 cells/ml). Following incubation with 10 µg of TCS at 4°C for 4 h, 0.5 ml aliquots of cells were washed with PBS, then incubated with rabbit anti-TCS antibody (1:1,000) in PBS containing 2% BSA at 4°C for 1 h. Specific binding of TCS was detected using FITC-conjugated antibody against rabbit IgG. The cells were analyzed by flow cytometry (FACScan, BD Bioscience). Basal cell fluorescence intensity was determined with cells stained with the secondary antibody alone. For the analysis of CCR5, anti-CCR5 antibody (CTC8) (10 µg) was incubated with cells at 4°C for 30 min before treatment with TCS.

Purification, Labeling of TCS and Binding Assay—TCS was purified from freshly harvested root tubes of *Trichosanthes kirilowii* Maximilwicz as previously described (23). Radioiodination of TCS was performed with Iodo-beads according to the supplier's instructions. The beads were rinsed twice with 50 mM Na₂HPO₄, pH 7.0, and dried. The beads were added to a solution of 10 µl of 125I (NaI, 1 mCi) diluted in 190 µl of 100 mM Na₂HPO₄, pH 7.0, and left at room temperature for 5 min. Then 20 µg of TCS dissolved in 10 µl of 100 mM Na₂HPO₄ was added.

After 20 min of incubation at room temperature, the solution was removed from the tube to terminate the reaction. Labeled TCS was separated from free iodine on a Sephadex G-25 column preequilibrated with PBS, pH 7.4, containing 0.2% BSA. Fractions of 0.5 ml were collected and the radioactivity was counted in a gamma counter.

Radioligand binding was carried out using intact Jar cells suspended in a binding buffer containing serum-free DMEM supplemented with 0.2% BSA following previously established methods (24–26). Typically, ¹²⁵I-TCS binding was carried out in a final volume of 0.5 ml of binding buffer containing 1×10^6 cells and different concentration of ¹²⁵I-TCS for 1 h at 4°C. Cell-bound radioactivity was recovered by rapid vacuum filtration through Whatman GF/B filter paper using a Brandel cell harvester. The filter paper was washed twice with 50 mM Tris-Cl, pH 7.4, containing 150 mM NaCl. Specific ¹²⁵I-binding was defined as the total binding less nonspecific binding. All measurements were made in triplicate via three independent experiments and were analyzed by the computer with program GraphPad Prism (GraphPad Software, Inc., USA).

Preparation of TCS- and BSA-Sepharose Beads—TCS and BSA were each conjugated to CNBr activated Sepharose beads according to the supplier's instructions. The fidelity of TCS-Sepharose beads was confirmed by application to the affinity purification of rabbit antibody against TCS.

Cell Surface Biotinylation—To identify TCS-binding proteins, live Jar cells were labeled with biotin following the supplier's instructions. In brief, 1×10^8 cells were harvested at the log phase of growth and washed three times with ice-cold PBS buffer (pH 8.0). Cells were then resuspended in 10 ml of the same buffer, and the cell surface proteins were labeled with biotin by addition of 10 mg of Sulfo-NHS-LC-biotin, followed by incubation at room temperature for 30 min with end-to-end rotation. The reaction was terminated by washing off excess free biotin with PBS/0.1% BSA.

Cell Extraction and Pull-Down—Jar cells labeled with biotin were lysed in 5 ml of cell lysis buffer (50 mM Tris-Cl, pH 7.4, 150 mM NaCl, 1 mM EDTA, 1% Triton X-100, and 1 mM PMSF) for 30 min on ice. The extract was centrifuged for 5 min at a speed of 12,000 rpm. The clarified supernatant was applied to an immobilized monomeric avidin column, and the bound biotinylated proteins were eluted with elution buffer (PBS, pH 7.4, 2 mM D-biotin) following the supplier's instructions. The biotinylated proteins purified by immobilized monomeric avidin were divided into aliquots corresponding to 2.5×10^7 cells and was pre-pulled-down with BSA-Sepharose beads at 4°C for 2 h. The supernatant was incubated with TCS-Sepharose beads at 4°C overnight, then washed with PBS. The precipitated proteins were eluted with the SDS sample buffer and boiled for 3 min before separation by SDS-PAGE. The proteins were then transferred onto immobilon-P membrane, followed by detection with HRP-conjugated streptavidin. For the analysis of sugar side chains or CCR5, the supernatant pre-pulled-down with BSA-Sepharose beads was incubated with Con A-Sepharose beads or anti-CCR5 antibody-conjugated protein G plus-agarose beads before being pulled down with TCS-Sepharose beads.

RT-PCR and Immunoblotting—For RT-PCR, total RNA was isolated from Jar and THP-1 cells with Trizol reagent (Promega). About 5 µg of total RNA was reversely

transcribed into cDNA (M-MLV Reverse Transcriptase, Promega), and 1/20 of the products was used in a 50- μ l PCR reaction. Conditions for the PCR reaction were: 94°C, 60 s; 94°C, 30 s, 60°C, 45 s, 72°C 60 s for 25 cycles, with a final extension for 10 m at 72°C. Primers used were as follows: 5'-atggatgatgatatcgcgcg-3' and 5'-aggattcctctgaccatg-3' for actin (27), 5'-tgctactcgggaatcataaaaact-3' and 5'-ttctgaacttctccccgacaaa-3' for CCR5 (28). To detect the expression of CCR5, Jar and THP-1 cells were collected and suspended with lysis buffer (50 mM Tris-Cl, pH 8.0, 150 mM NaCl, 1% Triton X-100, 100 μ g/ml PMSF, 1 mM EDTA). Proteins were separated by 10% SDS-PAGE and transferred onto immobilon-P membrane. Membranes were blocked for 1 h at room temperature in blocking buffer (TTBS, 2% BSA), then incubated with anti-CCR5 antibody (CTC8) (1:1,000) overnight at 4°C, rinsed and incubated for 1 h with a HRP-conjugated goat antibody against mouse IgG (1:1,000). Chemiluminescence detection was performed with ECL reagent.

RESULTS

Sensitivities of Choriocarcinoma Cells to TCS—The cytotoxicity of TCS to cells is summarized in Fig. 1. The 50% inhibitory dosage for TCS was around 5 μ g/ml for Jar cells, 7 μ g/ml for JEG-3, 100 μ g/ml for Wish and for RM-1. Both choriocarcinoma cell lines (Jar and JEG-3) appeared to be sensitive to TCS, which is consistent with the observation by radioactive precursors incorporation determination (6), suggesting that the selective sensitivity was probably related to certain inherent properties of choriocarcinoma cells.

Confocal Laser Scanning Microscopy Analysis of Intracellular Ca^{2+} Levels—Confocal microscopy was used to study the changes of $[Ca^{2+}]$ in Jar cells treated with TCS. Jar cells were untreated (A) or treated (B) with 25 μ g/ml TCS for 5 min. Images of fluo-3 fluorescence were collected by confocal laser scanning microscopy. Figure 2B reveals high fluo-3 fluorescence in the cells treated with TCS.

Specific Binding of TCS on Jar Cells—Using a cell surface-binding assay, we examined the interaction of TCS with Jar cells and Wish cells. In this assay, an

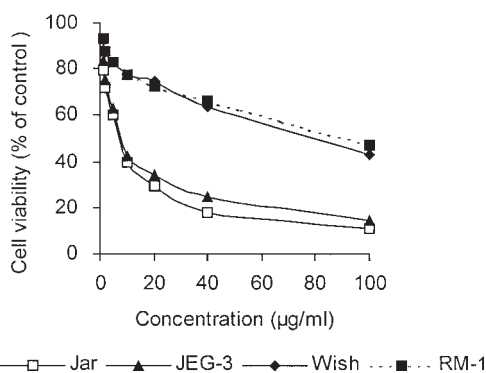


Fig. 1. Inhibitory effect of TCS on the growth of cultured cells. The cells were incubated with TCS for 48 h. The cell viability was measured by MTT assay. Growth inhibition is shown as the percentage of TCS-treated live cells to the control cultures. Each point is the mean of results obtained from three individual culture wells, and the standard deviation is less than 5%. The cell lines tested were Jar, JEG-3, Wish and RM-1.

FITC-conjugated antibody against rabbit IgG was used to detect the binding of TCS to these cells by flow cytometry. Figure 3 shows that the histogram was shifted to right when TCS was incubated with Jar cells. The shift was not seen when TCS was incubated with Wish cells. Thus, specific binding of TCS on Jar cells was detected.

Total radioactivity of ^{125}I -TCS was 5.6×10^7 cpm. Assuming 100% recovery, specific activity was approximately 2.8×10^6 cpm/ μ g. This value was used to estimate ^{125}I -TCS in all binding experiments.

Figure 4 shows the binding isotherm for TCS on Jar cells with Scatchard plot as an insert. A good curve fit was achieved for a model suggesting two classes of saturable binding sites for ^{125}I -TCS binding to Jar cells: a high affinity binding site ($B_{max1} = 10,351 \pm 2,400$ sites/cell, $K_{d1} = 0.2358 \pm 0.1$ nmol/liter) and a low affinity binding site ($B_{max2} = 102,037 \pm 31,500$ sites/cell, $K_{d2} = 10.41 \pm 3$ nmol/liter).

Two Binding Proteins Specific for TCS on Choriocarcinoma Cells—Rabbit anti-TCS polyclonal antibody was purified on an affinity column with immobilized TCS (Fig. 5A), which showed TCS-Sepharose beads worked very well.

Cell surface biotinylation and ECL detection was fast and as efficient as the radioactive assay involving cell

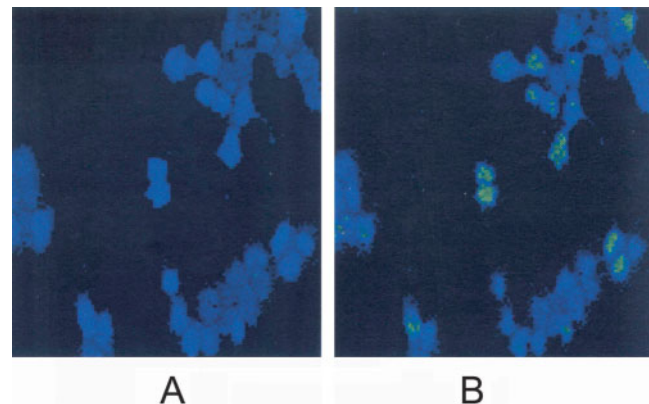


Fig. 2. Observation of the changes in intracellular Ca^{2+} concentration by confocal laser scanning microscopy. For measurement of $[Ca^{2+}]$, the cells were loaded with 5 μ M fluo-3/AM for 1 h at 37°C followed by the treatment with (B) or without (A) 25 μ g/ml TCS for 5 min.

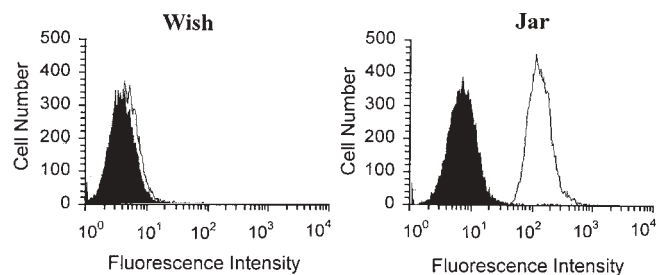


Fig. 3. FACS analysis of TCS binding onto Jar cells. Jar cells and Wish cells were incubated with TCS. The binding events were analyzed by flow cytometry. Results were presented as histograms of the log fluorescent intensities of 10^4 cells from the representative of three independent experiments. The unfilled histogram shows the staining of TCS, while the filled histogram indicates the basal cell fluorescence intensity.

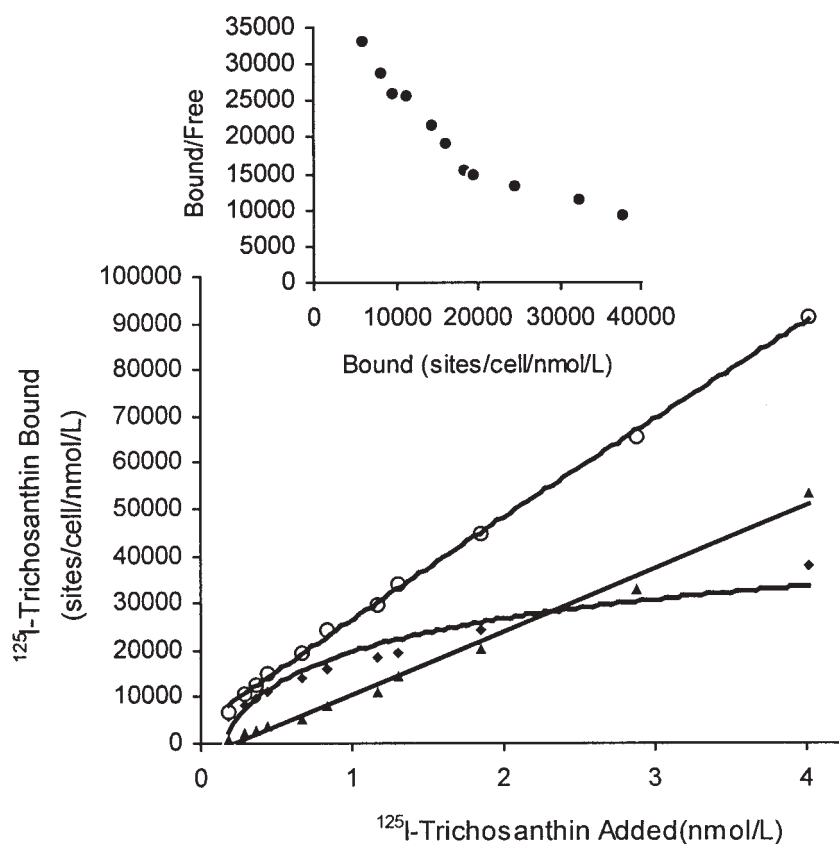


Fig. 4. Saturation experiments with ^{125}I -TCS binding on Jar cells. Intact cells (5×10^5 cells/500 μl) were incubated for 1 h at 4°C with 11 different concentrations of ^{125}I -TCS ranging from 0.1 to 4 nmol/liter in duplicate. Nonspecific binding was determined in the presence of 1 $\mu\text{mol/liter}$ TCS. Binding data were plotted according to Scatchard. SD for each data point was less than 10%. Parameters were calculated by computer analysis assuming two binding sites according to computer program GraphPad Prism. It showed a typical two-binding-sites model for intact Jar cells ($B_{\text{max}1} = 10,351 \pm 2,400$ sites/cell, $K_{d1} = 0.2358 \pm 0.1$ nmol/liter; $B_{\text{max}2} = 102,037 \pm 31,500$ sites/cell, $K_{d2} = 10.41 \pm 3$ nmol/liter). Diamonds: specific binding; triangles: non-specific binding; circles: total binding.

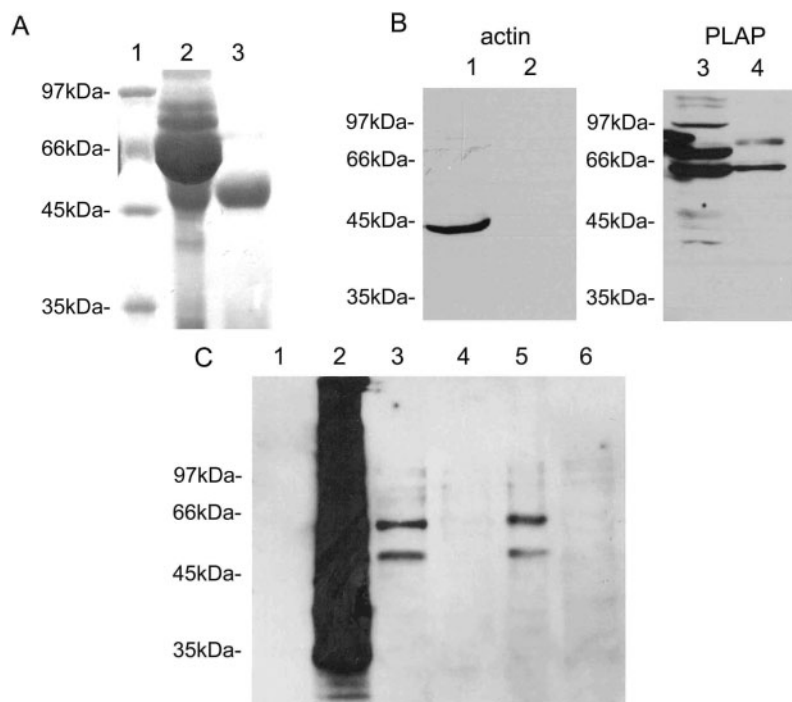


Fig. 5. Pull-down of TCS-binding proteins from Jar cells. (A) SDS-PAGE analysis of the affinity purification of anti-TCS antibody. Lane 1, protein markers; lane 2, rabbit anti-TCS antiserum; lane 3, purified antibody. (B) The biotinylated proteins were purified by use of immobilized monomeric avidin and detected with anti-actin antibody or anti-PLAP antibody. Lane 1, 3: total proteins from Jar cells; lane 2, 4: total membrane proteins purified by immobilized monomeric avidin. (C) Identification and characterization of TCS-binding proteins from Jar cells. The surface biotinylated proteins on Jar cells were purified by use of immobilized monomeric avidin and pre-pulled-down with BSA-Sepharose beads, then with anti-CCR5 antibody-conjugated protein G plus-agarose beads (lane 5) or Con A-Sepharose beads (lane 6) or without (lanes 3 and 4). The supernatants were pulled down with TCS-Sepharose beads, then washed with PBS (lanes 3, 5, and 6) or excessive TCS (lane 4). The precipitated proteins were separated by SDS-PAGE and transferred to Immobilon-P membrane, followed by detection with HRP-conjugated streptavidin. Lane 1, total proteins; lane 2, total biotinylated proteins purified by use of immobilized monomeric avidin.

surface labeling with ^{125}I (29, 30). In order to isolate TCS-binding proteins from Jar cells, membrane impermeable derivatives of biotin were used to label cytoplasmic membrane proteins. The biotinylated

membrane proteins were purified by immobilized monomeric avidin and pulled down with TCS-Sepharose beads. The precipitated proteins were separated by SDS-PAGE and transferred to blotting membrane, then

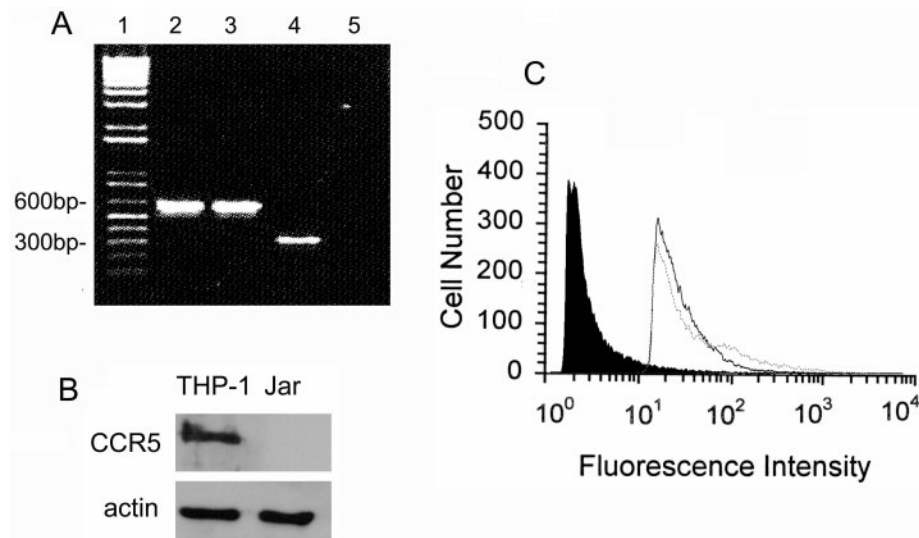


Fig. 6. CCR5 is not involved in the binding of TCS to Jar cells. (A) RT-PCR analysis of the expression of CCR5 in THP-1 and Jar cells. Lane 1, DNA marker; lane 2 and lane 3, actin for THP-1 cells and Jar cells; lane 4 and lane 5, CCR5 for THP-1 cells and Jar cells. (B) Western blotting analysis of the expression of CCR5 in THP-1 and Jar cells. (C) FACS analysis of TCS binding onto Jar cells. The unfilled histogram shows staining of TCS in the presence of anti-CCR5 antibody (—) or without (—), while the filled histogram indicates the basal cell fluorescence intensity.

visualized by probing with HRP-conjugated streptavidin. Figure 5C (lane 3) shows that TCS-Sepharose beads pulled down two proteins of 50 kDa and 60 kDa from Jar cells, which were regarded as the putative TCS binding proteins on the Jar cell membrane. Figure 5C (lane 4) showed that these two proteins could also be washed off TCS-Sepharose beads with an excess of TCS. As the positive control to show the fidelity of this assay, biotinylated PLAP (a membrane protein) was detectable (Fig. 5B, lane 4) by anti-PLAP polyclonal antibody in the biotinylated membrane proteins purified by use of immobilized monomeric avidin. But actin (non-membrane protein) was not biotinylated or detectable with anti-actin antibody (Fig. 5B, lane 2).

Con A displays high affinities to terminal α -D-mannosyl, α -D-glucosyl and sterically related residues (31, 32). When the biotinylated membrane proteins purified by immobilized monomeric avidin were pulled down with Con A-Sepharose beads before TCS-Sepharose beads, the two TCS-binding proteins disappeared (Fig. 5B, lane 6), which indicated that they could bind to ConA and thus contained sugar side chains.

CCR5 Is Not Involved in the Binding of TCS with Jar Cells—TCS specifically associated with beta-chemokine receptor CCR5 (17), of which the molecular mass was determined to be about 42 or 62 kDa (33). It is tempting to investigate whether the two binding proteins specific for TCS on choriocarcinoma cells were CCR5. RT-PCR and Western blotting analysis (Fig. 6, A and B) confirmed that Jar cells do not express CCR5, which is consistent with the previous report (28). CCR5 antibody (CTC8) recognized N-terminal epitopes of CCR5 and blocked HIV gp120 binding much more efficiently than chemokine (34). Figure 6C shows that CCR5 antibody did not interfere with the specific association of TCS with Jar cells. If the biotinylated membrane proteins purified by use of immobilized monomeric avidin were pre-pulled-down with anti-CCR5 antibody-conjugated protein G plus-agarose beads, two TCS-binding proteins could still be pulled down with TCS-Sepharose from the supernatant (Fig. 5B, lane 5), which indicated that CCR5 was not involved in the binding of TCS with Jar cells.

DISCUSSION

TCS exhibits a very broad spectrum of biological and pharmacological activities, including nuclease, protein-synthesis-inhibiting, immunosuppressive, abortifacient, anti-tumor and anti-human immunodeficiency virus activities (1–11), which might be dependent (2, 16) or independent of its RIP activity (17, 18, 35). The interaction between TCS and plasma membrane proteins is crucial for its cytotoxicity, but the nature of this interaction has remained elusive. This study was carried out to directly investigate the binding of TCS to the cells.

The choriocarcinoma cells were very sensitive to TCS (Fig. 1). The interaction between 125 I-labelled TCS with intact Jar cells was examined in this report. The corresponding Scatchard plots were curvilinear, which indicated two classes of binding sites on Jar cells: a high affinity binding site ($B_{max1} = 10,351 \pm 2,400$ sites/cell, $K_{d1} = 0.2358 \pm 0.1$ nmol/liter) and a low affinity binding site ($B_{max2} = 102,037 \pm 31,500$ sites/cell, $K_{d2} = 10.41 \pm 3$ nmol/liter). This specific binding was confirmed by flow cytometry analysis (Fig. 3), in which TCS binding was specifically detected on Jar cells. To identify the binding proteins to TCS, the best approach would be to isolate them from sensitive cells and characterize them. In this report, affinity beads with immobilized TCS were used to pull down the binding proteins to TCS from Jar cells. As a result, two proteins with molecular mass of 50 kDa and 60 kDa that specifically bind to TCS-Sepharose beads (Fig. 5C) were identified. These proteins could also be washed off TCS-Sepharose beads with excessive TCS, which suggested that these account for two classes of saturable binding sites for TCS on the Jar cell membrane (Fig. 4).

Some studies have indicated that TCS might enter the cell *via* the endocytic receptors such as low-density lipoprotein receptor-related protein and megalin, in order to exert its ribosome-inactivating effects inside the cell, in a way similar to saporin and ricin internalization (16). However, the selective cytotoxicity of TCS, such as its abortifacient, anti-HIV and anti-tumor activity, had not

been fully elucidated. Some RIPs showed various degrees of abortifacient activity, while others, such as ricin, did not (23). This study demonstrated that the two proteins specifically associated with TCS were clearly not low-density lipoprotein receptor-related protein or megalin, which have molecular masses of more than 200 kDa (16). Some TCS mutations designed to enhance its internalization by addition of amino acid sequences almost abolished its anti-HIV activity (35). Our previous study also revealed that some TCS mutants in which RIP activity was almost absent still retained some abortifacient activity (36). TCS could greatly stimulate chemotaxis and G protein activation of chemokines, mediated through functional interaction between TCS and chemokine receptors, independently of its RIP activity (17). All of the above studies may lead to the hypothesis that the abortifacient activity of TCS selectively injuring choriocarcinoma cells might involve a mechanism different from its *in vitro* non-specific inhibitory activity to protein synthesis.

In an earlier study, we have shown that TCS could activate G protein on the membrane of Jar cells by GTP γ S-binding assay (37). Our recent work indicates that TCS inhibits PKC activity (Li J, unpublished observations). Zhang *et al.* (18) showed that TCS stimulated the production of reactive oxygen species and induced the activation of caspase-3 in Jar cells. Though the molecular mechanism underlying the cytotoxicity of TCS is largely unknown, we have shown in this report that TCS leads to a transient increase of intracellular Ca²⁺ level (Fig. 2). Moreover, we demonstrated there are two binding proteins specific for TCS on the cytoplasmic membrane of Jar cells. These two proteins were neither low-density lipoprotein receptor-related protein and megalin nor CCR5. Further characterization of these two novel TCS-binding proteins might provide new insight into the mechanism involved in TCS's inducing-abortions, anti-tumor and anti-HIV activity.

REFERENCES

- Zhang, X.J. and Wang, J.H. (1986) Homology of trichosanthin and ricin A chain. *Nature* **321**, 477–478
- Zhang, J.S. and Liu, W.Y. (1992) The mechanism of action of trichosanthin on eukaryotic ribosomes—RNA N-glycosidase activity of the cytotoxin. *Nucleic Acids Res.* **20**, 1271–1275
- Jin, S.W., Sun, X.X., Wang, S.F., Tian, G.Y., Gu, Z.W., Qian, W.W., Liu, Y.Z., She, W.Y., Qian, R.Q., and Wang, Y. (1981) Physical and chemical properties of crystalline trichosanthin. *Acta Chim. Sin.* **39**, 917–926
- Wang, Y., Qian, R.Q., Gu, Z.W., Jin, S.W., Zhang, L.Q., Xia, Z.X., Tian, G.Y., and Ni, C.Z. (1986) Scientific evaluation of Tian Hua Fen (THF)—history, chemistry and application. *Pure Appl. Chem.* **58**, 789–798
- Lu, P.X. and Jin, Y.C. (1990) Trichosanthin in the treatment of hydatidiform mole: clinical analysis of 52 cases. *Chin. Med. J.* **103**, 183–185
- Tsao, S.W., Yan, K.T., and Yeung, H.W. (1986) Selective killing of choriocarcinoma cells in vitro by trichosanthin, a plant protein purified from root tubers of the Chinese medicinal herb *Trichosanthes kirilowii*. *Toxicol.* **24**, 831–840
- Chow, T.P., Feldman, R.A., Lovett, M., and Piatak, M. (1990) Isolation and DNA sequence of a gene encoding alpha-trichosanthin, a type I ribosome-inactivating protein. *J. Biol. Chem.* **265**, 8670–8674
- Shaw, P.C., Chan, W.L., Yeung, H.W., and Ng, T.B. (1994) Minireview: trichosanthin—a protein with multiple pharmacological properties. *Life Sci.* **55**, 253–262
- McGrath, M.S., Hwang, K.M., Caldwell, S.E., Gaston, I., Luk, K.C., Wu, P. Ng, V.L., Crowe, S., Daniels, J., and Marsh, J. (1989) GLQ223: an inhibitor of human immunodeficiency virus replication in acutely and chronically infected cells of lymphocyte and mononuclear phagocyte lineage. *Proc. Natl. Acad. Sci. USA* **86**, 2844–2848
- McGrath, M.S., Santulli, S., and Gaston, I. (1990) Effects of GLQ223 on HIV replication in human monocyte/macrophages chronically infected in vitro with HIV. *AIDS Res. Hum. Retroviruses* **6**, 1039–1043
- Liu, G.W., Liu, F.Y., Liu, Y.J., and Yu, S.H. (1985) A summary of 402 cases of termination early pregnancy with crystalline preparation of trichosanthin in *Advances in Chinese Medicinal Material Research* (Chang, H.M., Yeung, H.W., Tso, W.W., and Koo, A., eds.) pp. 327–329, World Scientific Publ., Singapore
- Wang, Y., Ju, R., Huang, J., and Hsu, K. (1976) Investigations on the injurious effects of the abortifacient trichosanthin to monkey placental villi. *Acta Zool. Sin.* **22**, 156–158
- Wang, Y.T., Hsu, K.C., and Chiang, W.S. (1978) The ultrastructural observations on the injurious effects of the abortifacient trichosanthin on monkey trophoblast. *Acta Biol. Exp. Sin.* **11**, 263–265
- Xiong, Y.Z., Pan, P., Xu, S.Y., Zhang, J., Wang, Y.H., Zuo, J., and Gu, Z. (1976) Study on the effects of trichosanthin on human trophoblast cells *in vitro*. *Acta Zool. Sin.* **22**, 172–175
- Lu, Y., Xia, X., and Sui, S. (2001) The interaction of trichosanthin with supported phospholipid membranes studied by surface plasmon resonance. *Biochim. Biophys. Acta* **1512**, 308–316
- Chan, W.L., Shaw, P.C., Tam, S.C., Jacobsen, C., Gliemann, J., and Nielsen, M.S. (2000) Trichosanthin interacts with and enters cells via LDL receptor family members. *Biochem. Biophys. Res. Commun.* **270**, 453–457
- Zhao, J., Ben, L.H., Wu, Y.L., Hu, W., Ling, K., Xin, S.M., Nie, H.L., Ma, L., and Pei, G. (1999) Anti-HIV agent trichosanthin enhances the capabilities of chemokines to stimulate chemotaxis and G protein activation, and this is mediated through interaction of trichosanthin and chemokine receptors. *J. Exp. Med.* **190**, 101–111
- Zhang, C., Gong, Y., Ma, H., An, C., Chen, D., and Chen, Z.L. (2001) Reactive oxygen species involved in trichosanthin-induced apoptosis of human choriocarcinoma cells. *Biochem. J.* **355**, 653–661
- Mosmann, T. (1983) Rapid colorimetric assay for cellular growth and survival: application to proliferation and cytotoxicity assays. *J. Immunol. Methods* **65**, 55–63
- Yamagishi, S., Yamada, M., Koshimizu, H., Takai, S., Hatanaka, H., Takeda, K., Ichijo, H., Shimoke, K., and Ikeuchi, T. (2003) Apoptosis-signal regulating kinase-1 is involved in the low potassium-induced activation of p38 mitogen-activated protein kinase and c-Jun in cultured cerebellar granule neurons. *J. Biochem.* **133**, 719–724.
- Radsak, M.P., Hilf, N., Singh-Jasuja, H., Braedel, S., Brossart, P., Rammensee, H.G., and Schild, H. (2003) The heat shock protein Gp96 binds to human neutrophils and monocytes and stimulates effector functions. *Blood* **101**, 2810–2815
- Ma, Y.Q. and Geng, J.G. (2002) Obligatory requirement of sulfation for P-selectin binding to human salivary gland carcinoma Acc-M cells and breast carcinoma ZR-75-30 cells. *J. Immunol.* **168**, 1690–1696
- Ke, Y.B., Chen, J.K., Nie, H.L., He, X.H., Ke, X.Y., and Wang, Y.H. (1997) Structure-function relationship of trichosanthin. *Life Sci.* **60**, 465–472

24. Yoshimura, T. and Leonard, E.J. (1990) Identification of high affinity receptors for human monocyte chemoattractant protein-1 on human monocytes. *J. Immunol.* **145**, 292–297
25. Cox, D. and Seki, J. (1998) Characterization of the binding of FK633 to the platelet fibrinogen receptor. *Thromb. Res.* **91**, 129–136
26. Anhaupl, T., Liebl, B., and Remien, J. (1988) Kinetic and equilibrium studies of (-)¹²⁵I-iodocyanopindolol binding to beta-adrenoceptors on human lymphocytes: evidence for the existence of two classes of binding sites. *J. Recept. Res.* **8**, 47–57
27. Ding, X.Z., Smallridge, R.C., Galloway, R.J., and Kiang, J.G. (1996) Rapid assay of HSF1 and HSF2 gene expression by RT-PCR. *Mol. Cell. Biochem.* **158**, 189–192
28. Douglas, G.C., Thirkill, T.L., Sideris, V., Rabieh, M., Trollinger, D., and Nuccitelli, R. (2001) Chemokine receptor expression by human syncytiotrophoblast. *J. Reprod. Immunol.* **49**, 97–114
29. Meier, T., Arni, S., Malarkannan, S., Poincelet, M., and Hoessli, D. (1992) Immunodetection of biotinylated lymphocyte-surface proteins by enhanced chemiluminescence: a nonradioactive method for cell-surface protein analysis. *Anal. Biochem.* **204**, 220–226
30. Altin, J.G. and Pagler, E.B. (1995) A one-step procedure for biotinylation and chemical cross-linking of lymphocyte surface and intracellular membrane-associated molecules. *Anal. Biochem.* **224**, 382–389
31. Gunther, G.R., Wang, J.L., Yahara, I., Cunningham, B.A., and Edelman, G.M. (1973) Concanavalin A derivatives with altered biological activities. *Proc Natl. Acad. Sci. USA* **70**, 1012–1016
32. Mogi, K., Takeshita, H., Yasuda, T., Nakajima, T., Nakazato, E., Kaneko, Y., Itoi, M., and Kishi, K. (2003) Carp hepatopancreatic DNase I: biochemical, molecular, and immunological properties. *J. Biochem.* **133**, 377–386
33. Suzuki, S., Miyagi, T., Chuang, L.F., Yau, P.M., Doi, R.H., and Chuang, R.Y. (2002) Chemokine receptor CCR5: polymorphism at protein level. *Biochem. Biophys. Res. Commun.* **296**, 477–483
34. Lee, B., Sharron, M., Blanpain, C., Doranz, B.J., Vakili, J., Setoh, P., Berg, E., Liu, G., Guy, H.R., Durell, S.R., Parmentier, M., Chang, C.N., Price, K., Tsang, M., and Doms, R.W. (1999) Epitope mapping of CCR5 reveals multiple conformational states and distinct but overlapping structures involved in chemokine and coreceptor function. *J. Biol. Chem.* **274**, 9617–9626
35. Wang, J.H., Nie, H.L., Huang, H., Tam, S.C., and Zheng, Y.T. (2003) Independency of anti-HIV-1 activity from ribosome-inactivating activity of trichosanthin. *Biochem. Biophys. Res. Commun.* **302**, 89–94
36. Nie, H.L., Cai, X., He, X., Xu, L., Ke, X., Ke, Y., and Tam, S.C. (1998) Position 120–123, a potential active site of trichosanthin. *Life Sci.* **62**, 491–500
37. Wu, Z.H., Nie, H.L., Lu, B., Wang, Q., and Ke, Y.B. (1999) Activation of G protein on the membrane of TCS-sensitive cells. *Acta Biol. Exp. Sin.* **32**, 151–156